applied sciences

MDPI

Article

Electrochemical Corrosion of Galvanized Steel in Binary Sustainable Concrete Made with Sugar Cane Bagasse Ash (SCBA) and Silica Fume (SF) Exposed to Sulfates

Laura Landa-Ruiz [1], Miguel Angel Baltazar-Zamora [1,*], Juan Bosch [2], Jacob Ress [2], Griselda Santiago-Hurtado [3,*], Victor Manuel Moreno-Landeros [3], Sabino Márquez-Montero [1], Ce Tochtli Méndez [1], Adan Borunda [4], César A. Juárez-Alvarado [5], José M. Mendoza-Rangel [5,*] and David. M. Bastidas [2,*]

[1] Facultad de Ingeniería Civil-Xalapa, Universidad Veracruzana, Lomas del Estadio S/N, Zona Universitaria, Xalapa C.P. 91000, Mexico; lalanda@uv.mx (L.L.-R.); smarquez@uv.mx (S.M.-M.); cmendez@uv.mx (C.T.M.)
[2] National Center for Education and Research on Corrosion and Materials Performance, NCERCAMP-UA, Dept. Chemical, Biomolecular, and Corrosion Engineering, The University of Akron, 302 E Buchtel Ave, Akron, OH 44325-3906, USA; jb394@zips.uakron.edu (J.B.); jtr45@zips.uakron.edu (J.R.)
[3] Facultad de Ingeniería Civil-Unidad Torreón, UADEC, Torreón C.P. 27276, Mexico; vmmorlan@gmail.com
[4] Centro de Investigación en Materiales Avanzados S.C., Chihuahua C.P. 31136, Mexico; adan.borunda@cimav.edu.mx
[5] Facultad de Ingeniería Civil, Universidad Autónoma de Nuevo León, Ave. Pedro de Alba S/N, Ciudad Universitaria, San Nicolás de los Garza C.P. 66450, Mexico; cesar.juarezal@uanl.edu.mx
* Correspondence: mbaltazar@uv.mx (M.A.B.-Z.); grey.shg@gmail.com (G.S.-H.); jmmr.rangel@gmail.com (J.M.M.-R.); dbastidas@uakron.edu (D.M.B.); Tel.: +52-2282-5252-94 (M.A.B.-Z.); +1-330-972-2968 (D.M.B.)

Citation: Landa-Ruiz, L.; Baltazar-Zamora, M.A.; Bosch, J.; Ress, J.; Santiago-Hurtado, G.; Moreno-Landeros, V.M.; Márquez-Montero, S.; Méndez, C.T.; Borunda, A.; Juárez-Alvarado, C.A.; et al. Electrochemical Corrosion of Galvanized Steel in Binary Sustainable Concrete Made with Sugar Cane Bagasse Ash (SCBA) and Silica Fume (SF) Exposed to Sulfates. *Appl. Sci.* **2021**, *11*, 2133. https://doi.org/10.3390/app11052133

Received: 20 January 2021
Accepted: 24 February 2021
Published: 28 February 2021

Abstract: This research evaluates the behavior corrosion of galvanized steel (GS) and AISI 1018 carbon steel (CS) embedded in conventional concrete (CC) made with 100% CPC 30R and two binary sustainable concretes (BSC1 and BSC2) made with sugar cane bagasse ash (SCBA) and silica fume (SF), respectively, after 300 days of exposure to 3.5 wt.% $MgSO_4$ solution as aggressive medium. Electrochemical techniques were applied to monitor corrosion potential (E_{corr}) according to ASTM C-876-15 and linear polarization resistance (LPR) according to ASTM G59 for determining corrosion current density (i_{corr}). E_{corr} and i_{corr} results indicate after more than 300 days of exposure to the sulfate environment (3.5 wt.% $MgSO_4$ solution), that the CS specimens embedded in BSC1 and BSC2 presented greater protection against corrosion in 3.5 wt.% $MgSO_4$ than the specimens embedded in CC. It was also shown that this protection against sulfates is significantly increased when using GS reinforcements. The results indicate a higher resistance to corrosion by exposure to 3.5 wt.% magnesium sulfate two times greater for BSC1 and BSC2 specimens reinforced with GS than the specimens embedding CS. In summary, the combination of binary sustainable concrete with galvanized steel improves durability and lifetime in service, in addition to reducing the environmental impact of the civil engineering structures.

Keywords: corrosion; binary sustainable concrete; galvanized steel; AISI 1018 steel; sugar cane bagasse ash; silica fume; sulfates

1. Introduction

A wide variety of materials are used in the construction industry, the most utilized of which is ordinary Portland cement (OPC), an essential raw material for the manufacture of hydraulic concrete. Unfortunately, the massive energy consumption and carbon dioxide emission that is generated during its manufacturing process has negative impacts on the environment, such as climate change. For instance, the manufacturing of 1 ton of OPC releases around 0.87–1 ton of CO_2, leading to a global contribution around 10% of the CO_2

the anthropogenic and 2–3% (4–5 GJ/ton) of energy consumption. CO_2 is emitted from the calcination process of limestone, the combustion of fuels in the furnace and from the generation of energy for electricity [1–3].

Although there is an impact on the environment generated by the manufacture of OPC, Hydraulic concrete is the most widely used construction material worldwide [4–6]. This is due to the great versatility it presents in its physical, mechanical and durability properties [7–11]. However, the problem of corrosion in reinforced concrete structures is a multimillion-dollar problem in India among other countries [12]. It is also of great interest because it is considered the main factor causing premature structure damage. Over time, significant damage might occur, compromising the structural integrity of civil works such as bridges, buildings, etc. [13–16].

Corrosion of steel in concrete consists of an electrochemical redox reaction in which the oxidation of iron takes place at the anode while oxygen reduction reaction takes place at the cathode. Corrosion of steel happens due to several factors that affect the passive layer formed by the steel in a high pH environment, compromising its stability. The main factors that promote this passivity breakdown are carbonation and the ingress of aggressive ions [17,18]. Chloride and sulfate ions are detrimental for reinforced concrete, deteriorating its structural integrity, reducing its lifetime and increasing the cost of maintenance of civil infrastructures [19–22]. These ions are considered the main cause of the corrosion initiation stage of reinforcing steel. They are present in the environment from sulphated soils or contaminated by agrochemicals, wastewater, de-icing salts and marine environment, among others [23–25]. Furthermore, they can also be found in elements of the concrete mix (aggregates, cement, water, additives) [26–30]. During the oxidation of the steel embedded in concrete, an increased internal pressure is promoted due to the increased volume of the corrosion products from steel. This generates internal stresses or forces on the surrounding concrete, causing cracking or fragmentation [31,32].

Several investigations have been carried out from various approaches in order to mitigate corrosion of steel in concrete. For instance, some have proposed higher quality concrete mixes, as well as the effects of concrete containing corrosion inhibitors [33–36]. Additional approaches include microencapsulated corrosion inhibitors [37], application of epoxy coatings [38–40], alternative reinforcement steels such as stainless steels [41–46] and galvanized steel [47–52]. Furthermore, various investigations have been developed where agro-industrial and industrial residues have been used as partial substitutes for OPC, known as supplemental cementitious materials (SCMs). SCM, when incorporated into the concrete, improves the resistance to aggressive ions via promoting a more dense and less permeable concrete matrix. This is due to the pozzolanic characteristics of these residues [53,54] and allows the production of concretes that are more resistant to chloride and sulfate ion ingress. Among the main SCMs that have demonstrated the highest corrosion resistance are silica fume, granulated blast furnace slag, fly ash, metakaolin, rice husk ash, and sugar cane bagasse ash [55–63].

Sugar cane bagasse ash (SCBA) as a partial substitute for OPC has shown considerable benefits when used for the preparation of concrete mixtures, significantly increasing its durability. These concretes made with SCBA are known in the scientific community as ecological concretes, sustainable concrete, green concretes or eco-friendly concretes [64–66]. This is due to the incorporation of the SCBA in replacement percentages ranging from 5% to 30%. This replacement has a direct impact on caring for the environment, first for using an agro-industrial waste, that in Mexico still does not have a specific use, and second for reducing the use of OPC, which means a reduction in CO_2 emissions. Although there are many works on the use of SCBA as a substitute for OPC to produce eco-friendly concretes, it is important to mention that work is being carried out for its application in the construction of sustainable roads [67,68]. This present a great opportunity in the countries where the highest production of this residue is generated.

This research evaluates the corrosion behavior of conventional concrete (CC) made with 100% CPC 30R and two binary sustainable concrete (BSC1 and BSC2) made with

SCBA and SF, BSC1 made with 10% SCBA as a substitute for CPC 30R and the second made with 10% SF as a substitute. Reinforcing steel rebars of AISI 1018 carbon steel (CS) and galvanized steel (GS) were embedded and exposed for more than 300 days to a sulfated medium (3.5% solution of $MgSO_4$). This concentration was used to simulate an aggressive environment that contains sulfates where civil works can be built based on reinforced concrete, such as the foundation soil, contact with wastewater and marine environments, among others. The results obtained from the corrosion current intensity (i_{corr}) in CC, BSC1 and BSC2, have allowed us to understand the corrosion kinetics of GS used as a reinforcement in eco-friendly concrete exposed to a sulfated medium. Furthermore, the enhanced corrosion resistance of these concretes would promote the use of agro-industrial and industrial waste to manufacture sustainable and ecological concretes that contribute to a sustainable development of our society.

2. Materials and Methods

2.1. Materials Used for Made Binary Sustainable Concrete

In this research, OPC concrete was used CPC 30R (NMX C-414 standard of the ONNCCE) [69], BSC1 and BSC2 used SCBA and SF as partial substitutes for CPC 30R in percentages of 10%, respectively. The SCBA was sampled from one of the boilers where the combustion temperature reached 750 °C. The SF used was purchased from a commercial supplier. The aggregates used were from banks located in the Region of Xalapa, Veracruz (Mexico), and likewise the mixing water used was tap water.

2.2. Dosage of Binary Sustainable Concretes

The dosage of concrete mixtures was carried out according to the method of ACI 211.1 [70]. This method is based on the quality of the concrete required, mainly considering the resistance to simple compression (f'_c) or w/c ratio, the settlement (workability or consistency), in addition to the characterization of the physical properties of the aggregates (sand and gravel). By knowing these parameters, it is possible to perform the necessary concrete dosage, which determines the quantity of materials (cement, water, gravel and sand). For the physical characterization of the aggregates, the tests are carried out according to ASTM standards [71–74]. Table 1 summarizes these characteristics of the aggregates.

Table 1. Results of the characterization of the aggregates.

Physical Properties of Materials	Aggregate	
	Coarse	Fine
Maximum Aggregate Size (mm)	19.05	-
Bulk Density (Unit Weight) (kg/m^3)	1372	-
Relative Density (Specific Gravity)	2.4	2.6
Absorption (%)	3.1	1.6
Fineness Modulus	-	2.8

Table 2 the shows the dosage used for each concrete mixture, the first from CC (100% CPC 30R), the second BSC1 (90% CPC 30R-10% SCBA) and third BSC2 (90% CPC 30R-10% SF). As indicated above, the concretes BSC1 and BSC2 were made with a 10% substitution of CPC 30R for 10% SCBA and 10% SF respectively, this substitution percentage has proven to be adequate to improve the physical, mechanical and durability properties of concrete in different studies [75–77]. Table 3 shows the chemical composition of both binder materials used as a substitute to the OPC obtained by X-ray fluorescence (XRF) analysis, which was provided by the supplier.

Table 2. Dosage of conventional concrete and binary sustainable concrete, (kg/m^3 of concrete, ratio w/c = 0.65).

Materials	CC (100% CPC 30R)	BSC-1 (90% CPC 30R-10% SCBA)	BSC-2 (90% CPC 30R-10%SF)
Water	205	205	205
Cement	315	283.5	283.5
SCBA	0	31.5	0
SF	0	0	31.5
Coarse aggregate	928	928	928
Fine aggregate	762	762	762

Table 3. Chemical composition of SCBA and SF obtained by XRF.

Material	Concentration (wt.%)									
	SO_3	MgO	SiO_2	Fe_2O_3	Al_2O_3	CaO	K_2O	Na_2O	Others	LOI
SCBA	0.4	−4.3	77.14	3.87	5.17	3.9	0.83	0.2	1.39	2.8
SF	0.33	0.40	92.26	1.57	0.79	0.43	1.31	0.38	–	–

2.3. Test to the Fresh and Hardened Conventional Concrete and Binary Sustainable Concretes

The tests for the characterization of the concrete mixtures in a fresh state were performed in accordance with the ONNCCE and ASTM standards, the slump by NMX-C-156-ONNCCE-2010 [78], temperature by ASTM C 1064/C1064M–08 [79], density by NMX-C-162-ONNCCE-2014 [80], and the compressive strength in accordance with the NMX-C-083-ONNCCE-2014 standard [81]. The obtained results are shown in Table 4. Figure 1 shows the compressive strength test setup used in this study.

Table 4. Physical properties conventional concrete and binary sustainable concretes.

Test	CC (100% CPC 30R)	BSC1 (90% CPC 30R-10% SCBA)	BSC2 (90% CPC 30R-10% SF)
Slump, mm	20	15	10
Temperature, °C	23.0	22.0	21.0
Density, kg/m^3	1896	1892	1916
Compressive strength, MPa	21.18	20.69	25.20

Figure 1. Experimental tests setup of compressive strength test of concrete.

2.4. Nomenclature of the Studied Specimens CC, BSC1 and BSC2

For the test specimens and in accordance with the parameters for this research, the nomenclature of the specimens for evaluation of corrosion has the following definitions, as show in Table 5:

Table 5. Nomenclature of specimens for evaluation of corrosion.

Conventional Concrete / Binary Sustainable Concretes	Test Environments			
	DI-Water		$MgSO_4$	
	CS	GS	CS	GS
CC (100% CPC 30R)	CC-W-CS	CC-W-GS	CC-MS- CS	CC-MS-GS
BSC1 (90% CPC 30R-10% SCBA)	BSC1-W-CS	BSC1-W-GS	BSC1-MS- CS	BSC1-MS-GS
BSC2 (90% CPC 30R-10% SF)	BSC2 -W-CS	BSC2-W-GS	BSC2-MS- CS	BSC2-MS-GS

- CC = Conventional concrete
- BSC1 = Binary sustainable concrete 1
- BSC2 = Binary sustainable concrete 2
- W = deionized water (DI-water) (control medium)
- MS = 3.5 wt.% $MgSO_4$ solution (aggressive medium)
- CS = AISI 1018 carbon steel
- GS = Galvanized steel

2.5. Characteristic of Test Specimens and Electrochemical Cell for the Monitoring of Corrosion

The reinforced concrete specimens were prisms with dimensions of 150 × 150 × 150 mm, as depicted in Figure 2. In each specimen were three bars of steel, two for the evaluation of the corrosion behavior (monitoring of E_{corr} and i_{corr}). The bars were of 3/8″ of diameter, the first of GS and the second of CS, these bars were used as working electrodes (WE), and the third was an AISI 314 SS steel bar as auxiliary electrode (AE), according to the ASTM G-59 standard [82]. The composition for the AISI 1018 CS and GS rebars is included in Tables 6 and 7, respectively. The galvanized process was performed according to ASTM A767, specifying a minimum thickness of 85–87 µm [83]. Typical coatings thickness for rebars is in the range of 110–120 µm [83]. The galvanizing process consists of the reaction of steel and molten zinc, producing a coating on top of the steel. This coating is composed of iron-zinc alloy layers such as gamma, delta and zeta that grow from the steel. The outermost layer is composed of pure zinc or eta phase. One advantage of galvanizing compared to typical coatings is that the bonding mechanism depends on the inter-alloying process between the steel and the molten zinc [84].

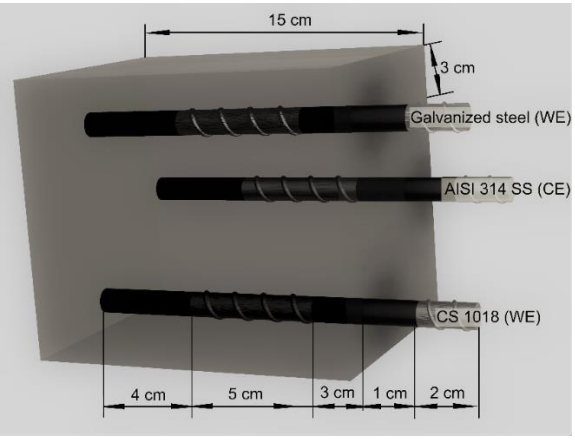

Figure 2. Dimensions of reinforced concrete specimens for electrochemical tests.

Table 6. Elemental composition (wt.%) of the AISI 1018 CS reinforcement tested.

Material	Element, wt.%									
	C	Si	Mn	P	S	Cr	Ni	Mo	Cu	Fe
AISI 1018	0.20	0.22	0.72	0.02	0.02	0.13	0.06	0.02	0.18	Balance

Table 7. Elemental composition (wt.%) of the zinc bath for the galvanizing process.

Al	Bi	Cd	Cu	Fe	Ni	Pb	Zn
0.003	0.007	0.0002	0.01	0.03	0.06	0.48	Balance

To evaluate the i_{corr}, linear polarization resistance (LPR) technique was applied. A three-electrode configuration was used consisting of the above mentioned WE and AW, and a copper/copper sulfate (CSE) reference electrode (RE), as depicted in Figure 3 [85,86]. The curing stage of all specimens was carried out by immersion in water for 28 days, according to NMX-C-159 standard [87]. After the curing period, the specimens were placed in two environments, DI-water (control medium) and 3.5 wt.% $MgSO_4$ solution (aggressive medium), the exposure time was for more than 300 days.

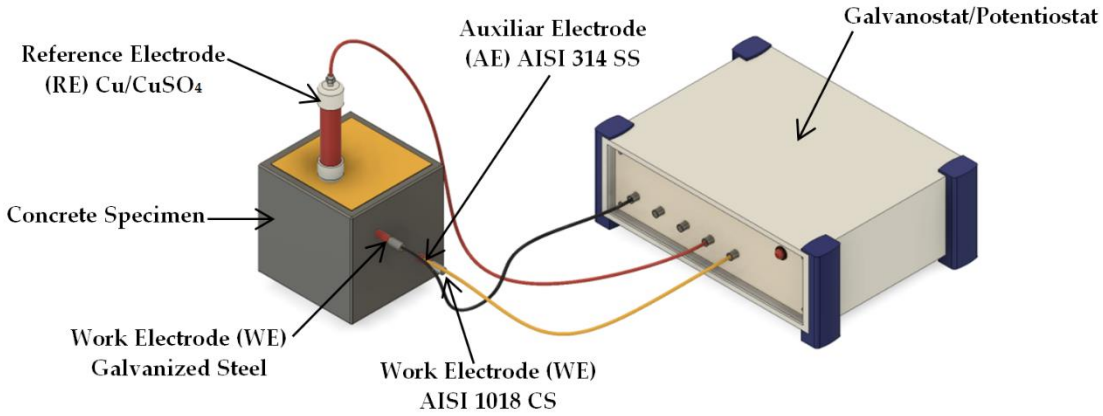

Figure 3. Electrochemical cell for the monitoring of corrosion.

A galvanostat/potentiostat Gill AC (ACM instruments) was used for corrosion monitoring (LPR), with a standard copper-copper sulfate ($Cu/CuSO_4$) as reference electrode. The parameters used to perform the LPR test were the same as those used by other researchers [88–90], the sweep potential was ±20 mV with respect to the corrosion potential and the sweep rate was 10 mV/minute, the IR drop potential was considered. The corrosion current density (i_{corr}) values were estimated from the polarization resistance (R_p) data using Stern and Geary equation (see Equation (1)):

$$i_{corr} = \frac{B}{R_p} \quad (1)$$

where B is Stern-Geary constant (B = 26 mV for carbon steel in active state) [91].

3. Results and Discussion

3.1. Corrosion Potential (E_{corr})

The E_{corr} of the specimens was monitored in accordance with ASTM C876-15 [92] and interpreted by the criteria presented in Table 8.

Table 8. Corrosion condition according to the measured corrosion potential (E_{corr}) versus a $Cu/CuSO_4$ (CSE) in reinforced concrete [92].

E_{corr} (mV vs. CSE)	Corrosion Condition
$E_{corr} > -200$	Low (10% of risk corrosion)
$-200 > E_{corr} > -350$	Intermediate corrosion risk
$-350 > E_{corr} > -500$	High (<90% of risk corrosion)
$E_{corr} < -500$	Severe Corrosion

3.1.1. E_{corr} Galvanized Steel and AISI 1018 Carbon Steel in Concrete Exposed to Control Medium (DI-Water)

In Figure 4, the behavior of corrosion potentials can be observed. E_{corr} of all study specimens when they were exposed to the control medium (water), both reinforced with galvanized steel, CC-W-GS, BSC1-W-GS and BSC2-W-GS as well as those reinforced with AISI 1018, CC-W-CS, BSC1-W-CS and BSC2-W-CS.

The difference in corrosion potentials according to the type of reinforcing steel is perfectly observed, the specimens with AISI 1018 CS present the most noble potentials, from the curing stage, with E_{corr} values ranging from –260 to –330 mV on day 7, reaching values lower than –200 mV after 28 days of curing, and afterwards displaying their most noble E_{corr} values at –110 mV until the end of the monitoring. This indicates, according to the ASTM C-876-15 standard, a 10% of risk corrosion in all specimens [92]. However, the specimen that presented the most positive or noble values was the BSC2-W-CS specimen, followed by BSC1-W-CS and CC-W-CS. In the case of specimens reinforced with galvanized steel, a similar behavior occurs, with E_{corr} values in the curing stage ranging from –800 to –1125 mV on day 7, and day 28 to E_{corr} values more positive, in a range from –680 to –880 mV, to continue with a passivation trend with values around –500 mV by day 98 and observing a slight increase in performance for the BSC2-W-GS and CC-W-GS specimens compared to that reported by the BSC1-W-GS specimen. The behavior of the E_{corr} values remains constant, indicating a 90% of risk corrosion until the end of the monitoring, with E_{corr} values between −500 to −350 mV for the three specimens. The results of the E_{corr} values of galvanized steel in the three concretes exposed to the control medium, agree with investigations where the corrosion efficiency of galvanized steel as reinforcement in concrete specimens was evaluated. In a study, initial corrosion potential values were recorded around −650mV, with differences of up to 100 mV between the study mixtures, associated with the difference in pH of the study mixtures as well as their water/cement ratio [93].

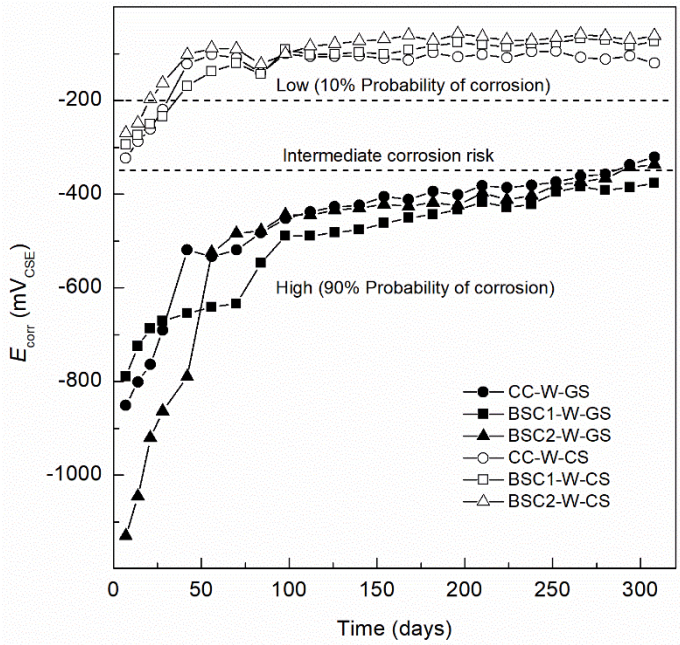

Figure 4. E_{corr} monitoring of GS and CS reinforced concrete exposed to control medium (DI-water).

3.1.2. E_{corr} Galvanized Steel and AISI 1018 Carbon Steel in Concrete Exposed to 3.5 wt.% $MgSO_4$ Solution

In Figure 5, the E_{corr} behavior of the studied specimens can be observed when exposed to the aggressive medium (3.5 wt.% $MgSO_4$ solution) for more than 300 days. In the curing stage, they present a behavior similar to that reported in the specimens exposed to the

control medium, with a passivation behavior on the three studied mixtures, presenting E_{corr} values in a range of −280 and −400 mV on day 7 for CC-MS-CS, BSC1-MS-CS and BSC2-MS-CS specimens. On the last day of the curing stage, day 28, E_{corr} values were found in the range of −240 and −290 mV. A passivation behavior of the corrosion potentials was observed towards more positive values until day 126 reaching values of −150 mV for the BSC1-MS-CS specimen, −170 mV for the BSC2-MS-CS and −210 mV for CC-MS-CS specimen. Later, a decreasing tendency is observed over time, reaching, at the end of the monitoring, values that indicate intermediate corrosion risk according to the ASTM C-876-15 standard with values of −348 mV for the CC-MS-CS specimen, −300 mV for the BSC1-MS-CS specimen and −280 mV for the BSC2-MS-CS specimen. A benefit from the use of binary sustainable concretes is observed, presenting a better performance against the corrosion in the presence of magnesium sulfate. Specifically, the specimen made with 10% Silica Fume (BSC2) showed enhanced corrosion resistance, followed by 10% SCBA (BSC1).

In the case of specimens with galvanized steel in the curing stage, a behavior similar to that reported in the specimens exposed to the control medium is presented. E_{corr} values in the range of −1150 mV to −750 mV are observed on day 7, increasing towards more positive values in the range of −580 mV to −730 mV on day 28, at the end of the curing stage. A passivation stage is also observed when exposed to the aggressive environment (3.5 wt.% $MgSO_4$ solution), according to the literature [94,95], said passivation period lasts until day 126, reaching values up to −355 mV for the CC-MS-GS specimen and −400 mV for the BSC1-MS-GS and BSC2-MS-GS specimens, to later present a trend towards more negative E_{corr} values, which remain stable from day 154 to 252 in a range between −400 and −440 mV, indicating 90% risk corrosion according to the ASTM C-876-15 standard [92]. Later, a pronounced tendency to more negative values is observed, associated with the depassivation or activation of the steel-concrete system, reaching values of −620 mV for the CC-MS-GS specimen, followed by the BSC1-MS-GS with an E_{corr} of −590 mV and the BSC2-MS-GS specimen with the best performance, with a corrosion potential of –510 mV at the end of the monitoring. The behavior indicates a better performance, evaluated according to what is indicated in the ASTM C-876-15 standard, of the binary sustainable concretes made with 10% SF, BSC2-MS-GS, followed by the one made with 10% SCBA, BSC1-MS-GS and finally the specimen made with 100% CPC 30R, CC-MS-GS [92].

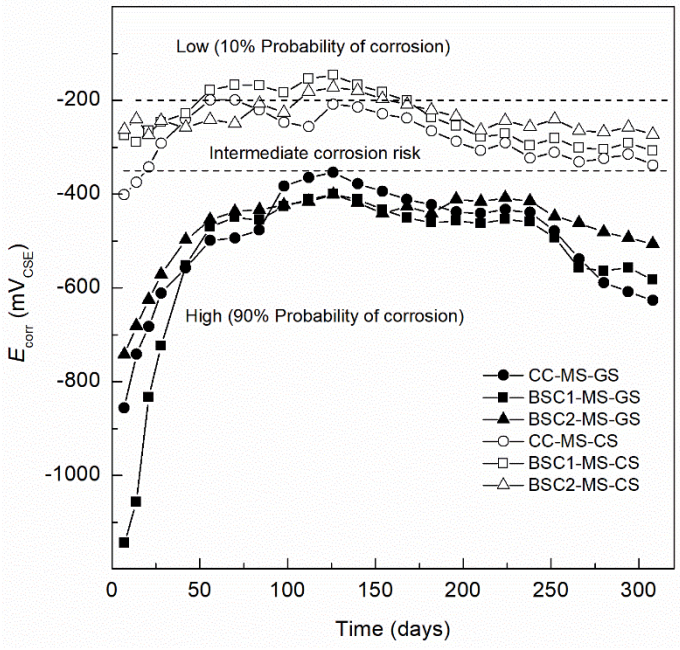

Figure 5. E_{corr} monitoring of GS and CS reinforced concrete exposed to 3.5 wt.% $MgSO_4$ solution.

3.2. Corrosion Current Density (i_{corr})

The criteria used to analyze the i_{corr} results are based on the state of corrosion of carbon steel in OPC reported in the literature [96], as shown in Table 9.

Table 9. Level of corrosion in accordance with the corrosion current density (i_{corr}) [96].

icorr (μA/cm2)	Corrosion Level
$i_{corr} \leq 0.1$	Negligible (Passivity)
$0.1 < i_{corr} < 0.5$	Low Corrosion
$0.5 < i_{corr} < 1$	Moderate Corrosion
$i_{corr} > 1$	High Corrosion

3.2.1. Behavior i_{corr} Galvanized Steel and AISI 1018 Carbon Steel in Concrete Exposed to Control Medium

Figure 6 shows the behavior of the corrosion rate or corrosion current intensity (i_{corr}) of the CC and binary sustainable concrete specimens immersed in a control medium (DI-Water), reinforced with CS and GS. All specimens with AISI 1018 CS present values of i_{corr} between 0.4 to 0.3 μA/cm^2 on day 7, progressively decreasing to values between 0.16 to 0.12 μA/cm^2 on day 28. This agrees with various works reported in the literature, associated with the progressive formation of a passivation layer in the steel rebars embedded in concrete during this period of time or curing stage [97,98]. As exposure time increases, a tendency of CC-W-CS, BSC1-W-CS and BSC2-W-CS to more noble values of i_{corr} is observed. BSC2-W-CS, which is made with binary sustainable concrete, shows the least active values. This specimen presents i_{corr} values below 0.10 μA/cm^2 since day 112, indicating a negligible level of corrosion according to Table 9. This trend maintains until the end of monitoring, when values of 0.04 μA/cm^2 are observed. The CC-W-CS and BSC1-W-CS specimens, which after day 182 present values of i_{corr} lower than 0.10 μA/cm^2, displayed very similar values, reaching i_{corr} values of 0.05 and 0.06 μA/cm^2 at the end of the monitoring, indicating a negligible level of corrosion.

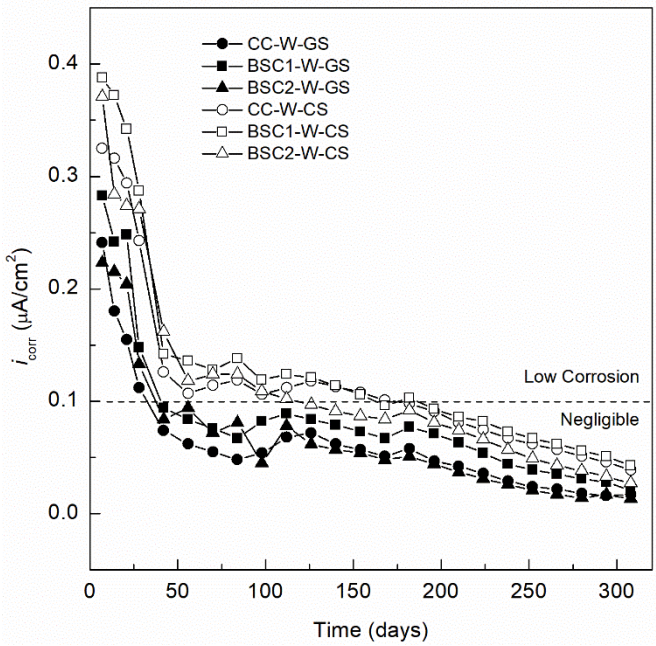

Figure 6. i_{corr} monitoring of GS and CS reinforced concrete exposed to control medium (DI-water).

For the specimens reinforced with GS, CC-W-GS, BSC1-W-GS and BSC2-W-GS the behavior is very similar, with high i_{corr} values at the beginning of the curing stage ranging from 0.28 and 0.23 μA/cm^2 on day 7, decreasing to values below 0.10 μA/cm^2 on day 28.

This behavior is associated with protection offered by the zinc layer of said steels, observed during the 300 days of monitoring. This is observed in the GS specimens that present lower values of i_{corr} than the specimens with AISI 1018 CS. It is also found that the specimen made with binary sustainable concrete, using 10% silica fume, BSC2-W-GS specimen, presents the noblest i_{corr} values than those reported by the CC-W-GS and BSC1-W-GS specimens. However, it is observed that all the specimens with GS, CC-W-GS, BSC1-W-GS and BSC2-W-GS presented i_{corr} values that indicate a negligible level of corrosion according to the Table 9, behavior that agrees with the results of other investigations [99,100], when evaluating corrosion in control media or media without aggressive agents such as sulfates or chlorides.

3.2.2. i_{corr} Galvanized Steel and AISI 1018 Carbon Steel in Concrete Exposed to 3.5 wt.% $MgSO_4$ Solution

Figure 7 shows the i_{corr} transient response of the CS and GS reinforcements embedded in CC, BSC1 and BSC2 exposed to 3.5 wt.% $MgSO_4$ solution. Specimens reinforced with CS, CC-MS-CS, BSC1-MS-CS and BSC2-MS-CS, present a behavior very similar to those reported in the reference specimens exposed to the control media during the curing stage, with i_{corr} values between 0.38 and 0.34 μA/cm^2, reaching values of i_{corr} between 0.32 and 0.25 μA/cm^2 on day 28. This is associated with the formation of the passive layer. When the specimen is exposed to the aggressive environment, the i_{corr} values show a decreasing tendency, with values below 0.10 μA/cm^2 on day 84, indicating a negligible level of corrosion in this moment. This behavior agrees with the literature, where a favorable behavior against corrosion occurs in the first months of exposure to sulfated media [101]. However, after day 126 of exposure, there is an increasing trend in the i_{corr} values for the three specimens, CC-MS-CS, BSC1-MS-CS and BSC2-MS-CS, which agrees with the E_{corr} values reported for specimens, which can be associated with the activation of the system. This activation is achieved on day 168 when the three specimens presented values greater than 0.10 μA/cm^2, remaining between 0.13 and 0.09 μA/cm^2, until day 252, where there is a greater increase in corrosion rate, reaching values of i_{corr} at the end of the monitoring of 0.24, 0.22 and 0.18 μA/cm^2, respectively. This indicates that in the exposure conditions of the present study, the CS reinforced BSC1 and BSC2 specimens impart a higher corrosion protection than CC, this favorable behavior coinciding with the use of SCBA and SF in sulfate media as reported in the literature [102].

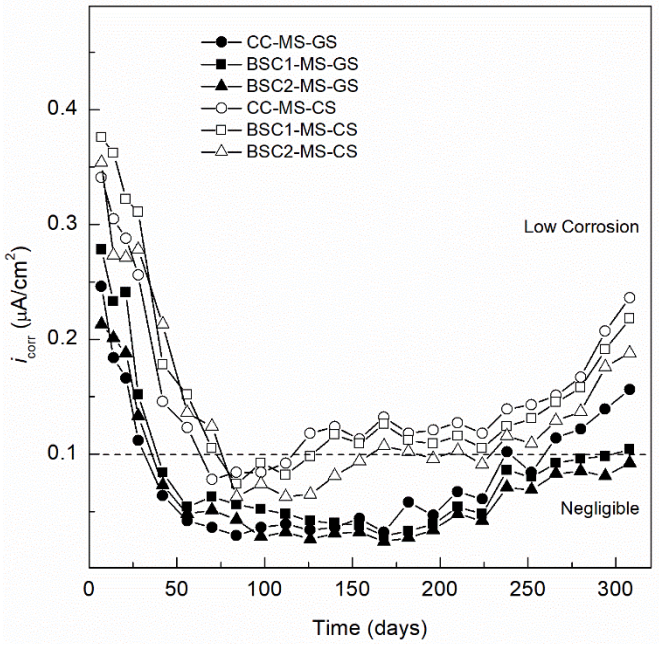

Figure 7. i_{corr} monitoring of GS and CS reinforced concrete exposed to 3.5 wt.% $MgSO_4$ solution.

The specimens with GS, CC-MS-GS, BSC1-MS-GS and BSC2-MS-GS also presented a behavior very similar to that analyzed in the specimens exposed to the control medium (DI-water) in the curing stage. Showing i_{corr} values between 0.28 and 0.22 μA/cm^2, at the beginning of the curing stage and reaching values of i_{corr} between 0.16 and 0.11 μA/cm^2 on day 28. A decreasing tendency is observed in the corrosion kinetics, maintaining values of i_{corr} between 0.07 and 0.04 μA/cm^2, from day 56 to day 168. Thus indicating a better performance than the specimens reinforced with AISI 1018 CS, whose passivity breakdown occurred after day 126.

The activation of steel for the specimens with GS is observed on day 182 with a constant increase, although still with i_{corr} values below 0.10 μA/cm^2, which indicates according to Table 9 that the level of corrosion is negligible. However, for the CC-MS-GS specimen, made with conventional concrete (100% CPC), an i_{corr} value above the passivation threshold is observed, showing an i_{corr} value of 0.12 μA/cm^2, associated with a moderate level of corrosion. An increasing trend in the i_{corr} values is observed, with an i_{corr} value of 0.16 μA/cm^2. In the case of specimens made with BSC1 and BSC2, there is a greater resistance to corrosion induced by sulfates, presenting the specimen BSC1-MS-GS made with SCBA values until day 294 below 0.10 μA/cm^2. However, in the last monitoring, it reached a value slightly higher than 0.10 μA/cm^2, indicating the activation of the system but higher resistance than the CC-MS-GS specimen. Likewise, the specimen that presented the best performance is the BSC2-MS-GS specimen, which at the end of the monitoring presented an increased trend, but without reaching values greater than 0.10 μA/cm^2, presenting a negligible level of corrosion throughout the exposure time. The benefit of the use of galvanized steel observed in the present investigation is greater, due to the exposure medium, but it has been shown that its anticorrosive efficiency decreases in the presence of chlorides, recommending its use in harsh environments that have up to a concentration of 1% of NaCl as reported in the literature [103]. Other studies evaluated the effect of carbonation on the corrosion of galvanized steel [104], where a protection period was also reported, the same was observed in an investigation where they used corrosion inhibitors applied to galvanized steel exposed in pore solution [105]. All of the above indicates that although galvanized steel protects against corrosion when used as reinforcing steel in concrete structures. The multiple possibilities of means of contact and life in service allow us to continue researching on the subject to increase its resistance to corrosion due to aggressive agents such as sulfates and chlorides, which are the most aggressive and main cause of corrosion in reinforced concrete structures, the most widely used construction system in the world. According to the results obtained in the present investigation, the use of agro-industrial and industrial residues (SCBA and SF), as partial substitutes for cement in the preparation of binary sustainable concretes, are an excellent option to increase resistance to corrosion by sulfates in addition to contribute to the decrease in CO_2 emissions due to the manufacture of OPC.

4. Conclusions

A greater corrosion resistance of the AISI 1018 carbon steel reinforcement was observed for specimens made with binary sustainable concretes based on SCBA and SF as a 10% replacement for OPC when exposed to sulfates compared to conventional concrete specimens.

The AISI 1018 CS reinforcements present an excellent corrosion performance in 3.5 wt.% $MgSO_4$ solution, showing E_{corr} values comprised between −200 mV_{CSE} and −350 mV_{CSE} after 300 days of exposure, indicating an intermediate probability of corrosion. GS reinforce samples showed a more active E_{corr} values around the −400 mV_{CSE}. Both binary sustainable concrete mixtures presented lower corrosion risk compare to conventional Portland cement matrices.

The corrosion current density values (i_{corr}) obtained for all reinforced samples after exposure to water for 300 days were below the corrosion threshold i_{corr} of 0.1 μA/cm^2. In addition, GS reinforced BSC1 and BSC2 samples exposed to 3.5 wt.% of $MgSO_4$ solution

showed a higher corrosion resistance during the same period of 300 days with i_{corr} values lower that 0.1 $\mu A/cm^2$, thus indicating a low corrosion risk.

A higher corrosion resistance to sulfate containing medium was observed with the combined use of binary sustainable concrete reinforced with GS compare to CS reinforcements, 0.1 and 0.2 $\mu A/cm^2$, respectively. Passivity along all the monitoring was observed for the galvanized steel specimens in the sustainable binary concretes, thus indicating an enhanced service lifetime in sulfated medium.

Future work is needed to better determine the corrosion mechanisms of these novel green concrete cementitious materials to promote the transition towards more eco-friendly binders. The enhanced performance against corrosion showed for these binary concrete mixtures justifies the need for further research, where the agro-industrial and industrial waste with pozzolanic properties can be used as substitutes for OPC for the elaboration of concrete mixtures that comply with mechanical properties and durability. This new trend in corrosion protection of reinforced concrete structures will allow for a reduction in CO_2 emissions caused by the cement industry.

Author Contributions: Conceptualization, M.A.B.-Z., G.S.-H., J.M.M.-R. and D.M.B.; Methodology, L.L.-R., V.M.M.-L., S.M.-M., C.T.M., M.A.B.-Z. and D.M.B.; Data Curation, L.L.-R., M.A.B.-Z., J.B., J.R., G.S.-H., A.B., C.A.J.-A., J.M.M.-R. and D.M.B.; Writing—Review and Editing, L.L.-R., M.A.B.-Z., J.B., J.R., G.S.-H., J.M.M.-R. and D.M.B.; Visualization: M.A.B.-Z. and D.M.B.; Supervision: M.A.B.-Z. and D.M.B.; Funding acquisition: M.A.B.-Z. and D.M.B. All authors have read and agreed to the published version of the manuscript.

Funding: This research was funded by PRODEP for the support granted by the SEP, to the Academic Body UV-CA-458 "Sustainability and Durability of Materials for Civil Infrastructure", within the framework of the 2018 Call for the Strengthening of Academic Bodies with IDCA 28593. J.B., J.R. and D.M.B., acknowledge funding from Firestone Research, grant number 639430 and The University of Akron.

Institutional Review Board Statement: Not applicable.

Informed Consent Statement: Not applicable.

Acknowledgments: The authors thank PRODEP for the support granted by the SEP, to the Academic Body UV-CA-458 "Sustainability and Durability of Materials for Civil Infrastructure", within the framework of the 2018 Call for the Strengthening of Academic Bodies with IDCA 28593. The authors also thank A.E. Landa-Gómez for the technical support.

Conflicts of Interest: The authors declare no conflict of interest.

References

1. Worrell, E.; Price, L.; Martin, N.; Hendriks, C.; Ozawa, L.M. Carbon dioxide emissions from the global cement industry. *Annu. Rev. Energy Environ.* **2001**, *26*, 303–329. [CrossRef]
2. Monteiro, P.; Miller, S.; Horvath, A. Towards sustainable concrete. *Nat. Mater.* **2017**, *16*, 698–699. [CrossRef]
3. Mahasenan, N.; Smith, S.; Humphreys, K. The cement industry and global climate change current and potential future cement Industry CO_2 emissions. In Proceedings of the Greenhouse Gas Control Technologies—6th International Conference, Kyoto, Japan, 1–4 October 2002; Elsevier: Amsterdam, The Netherlands, 2003; pp. 995–1000.
4. Landa, A.; Croche, R.; Márquez-Montero, S.; Galván-Martínez, R.; Tiburcio, C.G.; Almeraya Calderón, F.; Baltazar, M. Correlation of compression resistance and rupture module of a concrete of ratio w/c= 0.50 with the corrosion potential, electrical resistivity and ultrasonic pulse speed. *ECS Trans.* **2018**, *84*, 217–227. [CrossRef]
5. Harilal, M.; Rathish, V.R.; Anandkumar, B.; George, R.P.; Haji, M.S.; Philip, J.; Amarendra, G. High performance green concrete (HPGC) with improved strength and chloride ion penetration resistance by synergistic action of fly ash, nanoparticles and corrosion inhibitor. *Constr. Build. Mater.* **2019**, *198*, 299–312. [CrossRef]
6. Landa, L.; Ariza, H.; Santiago, G.; Moreno, V.; López, R.; Villegas, R.; Márquez, S.; Croche, R.; Baltazar, M. Evaluation of the behavior of the physical and mechanical properties of green concrete exposed to magnesium sulfate. *Eur. J. Eng. Res. Sci.* **2020**, *5*, 1353–1356. [CrossRef]
7. Cramer, S.D.; Covino, B.S., Jr.; Bullard, S.J.; Holcomb, G.R.; Russell, J.H.; Nelson, F.J.; Laylor, H.M.; Soltesz, S.M. Corrosion prevention and remediation strategies for reinforced concrete coastal bridge. *Cem. Concr. Compos.* **2002**, *24*, 101–117. [CrossRef]

8. Santiago, G.; Maldonado-Bandala, E.E.; Olguin Coca, F.J.; Almeraya-Calderón, F.; Torres-Acosta, A.; Baltazar-Zamora, M.A. Electrochemical behavior of reinforced concrete and its relation with the environment of Xalapa, Veracruz. *Int. J. Electrochem. Sci.* **2012**, *7*, 9825–9834.
9. Raczkiewicz, W.; Wójcicki, A. Temperature impact on the assessment of reinforcement corrosion risk in concrete by galvanostatic pulse method. *Appl. Sci.* **2020**, *10*, 1089. [CrossRef]
10. Volpi-León, V.; López-Léon, L.D.; Hernández-Ávila, J.; Baltazar-Zamora, M.A.; Olguín-Coca, F.J.; López-León, A.L. Corrosion study in reinforced concrete made with mine waste as mineral additive. *Int. J. Electrochem. Sci.* **2017**, *12*, 22–31. [CrossRef]
11. Chalhoub, C.; François, R.; Carcasses, M. Critical chloride threshold values as a function of cement type and steel surface condition. *Cem. Concr. Res.* **2020**, *134*, 106086. [CrossRef]
12. Sudheer, S.; Raghu Babu, U.; Kondraivendhan, B. Influence of metakaolin and red mud blended cement on reinforcement corrosion in presence of chloride and sulfate ions. *Sustain. Constr. Build. Mater.* **2019**, *25*, 717–725.
13. Troconis de Rincón, O.; Montenegro, J.C.; Vera, R.; Carvajal, A.M.; De Gutiérrez, R.M.; Del Vasto, S.; Saborio, E.; Torres-Acosta, A.; Pérez-Quiroz, J.; Martínez-Madrid, M.; et al. Reinforced Concrete Durability in Marine Environments DURACON Project: Long-Term Exposure. *Corrosion* **2016**, *72*, 824–833. [CrossRef]
14. Liang, M.T.; Lan, J.-J. Reliability analysis for the existing reinforced concrete pile corrosion of bridge substructure. *Cem. Concr. Res.* **2005**, *35*, 540–550. [CrossRef]
15. Baltazar, M.A.; Márquez, S.; Landa, L.; Croche, R.; López, O. Effect of the type of curing on the corrosion behavior of concrete exposed to urban and marine environment. *Eur. J. Eng. Technol. Res.* **2020**, *5*, 91–95. [CrossRef]
16. Santiago-Hurtado, G.; Baltazar-Zamora, M.A.; Olguín-Coca, J.; López, L.D.; Galván-Martínez, R.; Ríos-Juárez, A.; Gaona-Tiburcio, C.; Almeraya-Calderón, F. Electrochemical evaluation of a stainless steel as reinforcement in sustainable concrete exposed to chlorides. *Int. J. Electrochem. Sci.* **2016**, *11*, 2994–3006. [CrossRef]
17. Bastidas, D.M.; Cobo, A.; Otero, E.; González, J.A. Electrochemical rehabilitation methods for reinforced concrete structures: Advantages and pitfalls. *Corros. Eng Sci. Technol.* **2008**, *43*, 248–255. [CrossRef]
18. Bastidas, D.M.; González, J.A.; Feliu, S.; Cobo, A.; Miranda, J.M. A quantitative study of concrete-embedded steel corrosion using potentiostatic pulses. *Corrosion* **2007**, *63*, 1094–1100. [CrossRef]
19. Cosoli, G.; Mobili, A.; Giulietti, N.; Chiariotti, P.; Pandarese, G.; Tittarelli, F.; Bellezze, T.; Mikanovic, N.; Revel, G.M. Performance of concretes manufactured with newly developed low-clinker cements exposed to water and chlorides: Characterization by means of electrical impedance measurements. *Constr. Build. Mater.* **2020**, *271*, 121546. [CrossRef]
20. Pham, V.T.; Meng, P.; Trinh Bui, P.; Ogawa, Y.; Kawai, K. Effects of Shirasu natural pozzolan and limestone powder on the strength and aggressive chemical resistance of concrete. *Constr. Build. Mater.* **2020**, *239*, 117679. [CrossRef]
21. Dalla, P.T.; Tragazikis, I.K.; Exarchos, D.A.; Konstantinos, G.; Dassios, K.G.; Barkoula, N.M.; Matikas, T.E. Effect of carbon nanotubes on chloride penetration in cement mortars. *Appl. Sci.* **2019**, *9*, 1032. [CrossRef]
22. Gyeongcheol, C.G.; Shinohara, Y.; Kim, G.; Lee, S.; Lee, E.; Nam, J. Concrete corrosion cracking and transverse bar strain behavior in a reinforced concrete column under simulated marine conditions. *Appl. Sci.* **2020**, *10*, 1794.
23. Santiago-Hurtado, G.; Baltazar-Zamora, M.A.; Galindo, D.A.; Cabral, M.J.A.; Estupiñán, L.F.H.; Zambrano, P.; Gaona-Tiburcio, C. Anticorrosive efficiency of primer applied in carbon steel AISI 1018 as reinforcement in a soil Type MH. *Int. J. Electrochem. Sci.* **2013**, *8*, 8490–8501.
24. Ismail, A.I.M.; El-Shamy, A.M. Engineering behaviour of soil materials on the corrosion of mild steel. *Appl. Clay Sci.* **2009**, *42*, 356–362. [CrossRef]
25. Liu, J.; Liu, J.; Huang, Z.; Zhu, J.; Liu, W.; Zhang, W. Effect of fly ash as cement replacement on chloride diffusion, chloride binding capacity, and micro-properties of concrete in a water soaking environment. *Appl. Sci.* **2020**, *10*, 6271. [CrossRef]
26. Anacta, E.T. Effect of salt-contaminated mixing water and aggregates on time-to-initiate rebar corrosion in concrete. *Int. J. Sci. Eng. Res.* **2013**, *4*, 1524–1527.
27. Raczkiewicz, W.; Kossakowski, P.G. Electrochemical diagnostics of sprayed fiber-reinforced concrete corrosion. *Appl. Sci.* **2019**, *9*, 3763. [CrossRef]
28. Dousti, A.; Moradian, M.; Taheri, S.; Rashetnia, R.; Shekarchi, M. Corrosion assessment of RC deck in a Jetty structure damaged by chloride attack. *J. Pelform. Constr. Facil.* **2013**, *27*, 519–528. [CrossRef]
29. Xu, P.; Jiang, L.; Guo, M.; Zha, J.; Chen, L.; Chen, C.; Xu, N. Influence of sulfate salt type on passive film of steel in simulated concrete pore solution. *Constr. Build. Mater.* **2019**, *223*, 352–359. [CrossRef]
30. Wang, D.; Zhao, X.; Meng, Y.; Chen, Z. Durability of concrete containing fly ash and silica fume against combined freezing-thawing and sulfate attack. *Constr. Build. Mater.* **2017**, *147*, 398–406. [CrossRef]
31. Cheng, A.; Huang, R.; Wu, J.K.; Chen, C.H. Effect of rebar coating on corrosion resistance and bond strength of reinforced concrete. *Constr. Build. Mater.* **2005**, *19*, 404–412. [CrossRef]
32. Bastidas, D.M.; Ress, J.; Martin, U.; Bosch, J.; La Iglesia, A.; Bastidas, J.M. Crystallization pressure and volume variation during rust development in marine and urban-continental environments: Critical factors influencing exfoliation. *Rev. Metal* **2020**, *56*, e164. [CrossRef]
33. Burtuujin, G.; Son, D.; Jang, I.; Yi, C.; Lee, H. Corrosion behavior of pre-rusted rebars in cement mortar exposed to harsh environment. *Appl. Sci.* **2020**, *10*, 8705. [CrossRef]

34. Coppola, L.; Coffetti, D.; Crotti, E.; Gazzaniga, G.; Pastore, T. Chloride diffusion in concrete protected with a silane-based corrosion inhibitor. *Materials* **2020**, *13*, 2001. [CrossRef] [PubMed]
35. Pan, C.; Li, X.; Mao, J. The effect of a corrosion inhibitor on the rehabilitation of reinforced concrete containing sea sand and seawater. *Materials* **2020**, *13*, 1480. [CrossRef] [PubMed]
36. Bastidas, D.M.; La Iglesia, V.M.; Criado, M.; Fajardo, S.; La Iglesia, A.; Bastidas, J.M. A prediction study of hydroxyapatite entrapment ability in concrete. *Constr. Build. Mater.* **2010**, *24*, 2646–2649. [CrossRef]
37. Ress, J.; Martin, U.; Bosch, J.; Bastidas, D.M. pH-triggered release of $NaNO_2$ corrosion inhibitors from novel colophony microcapsules in simulated concrete pore solution. *ACS Appl. Mater. Interfaces* **2020**, *12*, 46686–46700. [CrossRef]
38. Yeomans, S.R. Performance of black, galvanized, and epoxy-coated reinforcing steels in chloride-contaminated concrete. *Corrosion* **1994**, *50*, 72–81. [CrossRef]
39. Figueira, R.B. Electrochemical sensors for monitoring the corrosion conditions of reinforced concrete structures: A review. *Appl. Sci.* **2017**, *7*, 1157. [CrossRef]
40. Ress, J.; Martin, U.; Bosch, J.; Bastidas, D.M. Protection of carbon steel rebars by epoxy coating with smart environmentally friendly microcapsules. *Coatings* **2021**, *11*, 113. [CrossRef]
41. Fajardo, S.; Bastidas, D.M.; Criado, M.; Romero, M.; Bastidas, J.M. Corrosion behaviour of a new low-nickel stainless steel in saturated calcium hydroxide solution. *Constr. Build. Mater.* **2011**, *25*, 4190–4196. [CrossRef]
42. Baltazar, M.A.; Bastidas, D.M.; Santiago, G.; Mendoza, J.M.; Gaona, C.; Bastidas, J.M.; Almeraya, F. Effect of silica fume and fly ash admixtures on the corrosion behavior of AISI 304 embedded in concrete exposed in 3.5% NaCl solution. *Materials* **2019**, *12*, 4007. [CrossRef]
43. Fajardo, S.; Bastidas, D.M.; Ryan, M.P.; Criado, M.; McPhail, D.S.; Morris, R.J.H.; Bastidas, J.M. Low energy SIMS characterization of passive oxide films formed on a low-nickel stainless steel in alkaline media. *Appl. Surf. Sci.* **2014**, *288*, 423–429. [CrossRef]
44. Bautista, A.; Blanco, G.; Velasco, F. Corrosion behavior of low-nickel austenitic stainless steels reinforcements: A comparative study in simulated pore solutions. *Cem. Concr. Res.* **2006**, *36*, 1922–1930. [CrossRef]
45. Fajardo, S.; Bastidas, D.M.; Criado, M.; Bastidas, J.M. Electrochemical study on the corrosion behavior of a new low-nickel stainless steel in carbonated alkaline solution in the presence of chlorides. *Electrochim. Acta* **2014**, *129*, 160–170. [CrossRef]
46. Martin, U.; Ress, J.; Bosch, J.; Bastidas, D.M. Stress corrosion cracking mechanism of AISI 316LN stainless steel rebars in chloride contaminated concrete pore solution using the slow strain rate technique. *Electrochim. Acta* **2020**, *335*, 135565. [CrossRef]
47. Bellezze, T.; Malavolta, M.; Quaranta, A.; Ruffini, N.; Roventi, G. Corrosion behaviour in concrete of three differently galvanized steel bars. *Cem. Concr. Compos.* **2006**, *28*, 246–255. [CrossRef]
48. Tittarelli, F.; Mobili, A.; Giosuè, C.; Belli, A.; Bellezze, T. Corrosion behaviour of bare and galvanized steel in geopolymer and Ordinary Portland Cement based mortars with the same strength class exposed to chlorides. *Corros. Sci.* **2018**, *134*, 64–77. [CrossRef]
49. Kayali, O.; Yeomans, S.R. Bond of ribbed galvanized reinforcing steel in concrete. *Cem. Concr. Compos.* **2000**, *22*, 459–467. [CrossRef]
50. Baltazar, M.A.; Maldonado, M.; Tello, M.; Santiago, G.; Coca, F.; Cedano, A.; Barrios, C.P.; Nuñez, R.; Zambrano, P.; Gaona, C.; et al. Efficiency of galvanized steel embedded in concrete previously contaminated with 2, 3 and 4% of NaCl. *Int. J. Electrochem. Sci.* **2012**, *7*, 2997–3007.
51. Farhangi, V.; Karakouzian, M. Effect of fiber reinforced polymer tubes filled with recycled materials and concrete on structural capacity of pile foundations. *Appl. Sci.* **2020**, *10*, 1554. [CrossRef]
52. Baltazar, M.A.; Santiago, G.; Moreno, V.M.; Croche, R.; De la Garza, M.; Estupiñan, F.; Zambrano, P.; Gaona, G. Electrochemical behaviour of galvanized steel embedded in concrete exposed to sand contaminated with NaCl. *Int. J. Electrochem. Sci.* **2016**, *11*, 10306–10319. [CrossRef]
53. Muralidharan, S.; Parande, A.K.; Saraswathy, V.; Kumar, K.; Palaniswamy, N. Corrosion of steel in concrete with and without silica fume. *Zaštita Mater.* **2008**, *49*, 3–8.
54. Tibbetts, C.M.; Paris, J.M.; Ferraro, C.C.; Riding, K.A.; Townsend, T.G. Relating water permeability to electrical resistivity and chloride penetrability of concrete containing different supplementary cementitious materials. *Cem. Concr. Compos.* **2020**, *107*, 103491. [CrossRef]
55. Manera, M.; Vennesland, O.; Bertolini, L. Chloride threshold for rebar corrosion in concrete with addition of silica fume. *Corros. Sci.* **2008**, *50*, 554–560. [CrossRef]
56. Baltazar, M.A.; Ariza, H.; Landa, L.; Croche, R. Electrochemical evaluation of AISI 304 SS and galvanized steel in ternary ecological concrete based on sugar cane bagasse ash and silica fume (SCBA-SF) exposed to Na_2SO_4. *Eur. J. Eng. Res. Sci.* **2020**, *5*, 353–357. [CrossRef]
57. Heniegal, A.M.; Amin, M.; Youssef, H. Effect of silica fume and steel slag coarse aggregate on the corrosion resistance of steel bars. *Constr. Build. Mater.* **2017**, *155*, 846–851. [CrossRef]
58. Corinaldesi, V.; Donnini, J.; Giosué, C.; Mobili, A.; Tittarelli, F. Durability assessment of recycled aggregate HVFA concrete. *Appl. Sci.* **2020**, *10*, 6454. [CrossRef]
59. Gbozee, M.; Zheng, K.; Fuqiang, H.; Zenga, X. The influence of aluminum from metakaolin on chemical binding of chloride ions in hydrated cement pastes. *Appl. Clay Sci.* **2018**, *158*, 186–194. [CrossRef]

60. Padhi, R.; Mukharjee, B. Effect of rice husk ash on compressive strength of recycled aggregate concrete. *J. Basic Appl. Eng. Res.* **2017**, *4*, 356–359.
61. Khan, K.; Ullah, M.; Shahzada, K.; Amin, M.N.; Bibi, T.; Wahab, N.; Aljaafari, A. Effective use of micro-silica extracted from rice husk ash for the production of high-performance and sustainable cement mortar. *Constr. Build. Mater.* **2020**, *258*, 119589. [CrossRef]
62. Amin, N. Use of bagasse ash in concrete and its impact on the strength and chloride resistivity. *J. Mater. Civ. Eng.* **2011**, *23*, 717–720. [CrossRef]
63. Joshaghani, A.; Moeini, M.A. Evaluating the effects of sugar cane bagasse ash (SCBA) and nanosilica on the mechanical and durability properties of mortar. *Constr. Build. Mater.* **2017**, *152*, 818–831. [CrossRef]
64. Baltazar, M.A.; Landa, A.; Landa, L.; Ariza, H.; Gallego, P.; Ramírez, A.; Croche, R.; Márquez, S. Corrosion of AISI 316 stainless steel embedded in sustainable concrete made with sugar cane bagasse ash (SCBA) exposed to marine environment. *Eur. J. Eng. Res. Sci.* **2020**, *5*, 127–131. [CrossRef]
65. Ariza-Figueroa, H.A.; Bosch, J.; Baltazar-Zamora, M.A.; Croche, R.; Santiago-Hurtado, G.; Landa-Ruiz, L.; Mendoza-Rangel, J.M.; Bastidas, J.M.; Almeraya-Calderón, F.A.; Bastidas, D.M. Corrosion behavior of AISI 304 stainless steel reinforcements in SCBA-SF ternary ecological concrete exposed to $MgSO_4$. *Materials* **2020**, *13*, 2412. [CrossRef] [PubMed]
66. Landa-Sánchez, A.; Bosch, J.; Baltazar-Zamora, M.A.; Croche, R.; Landa-Ruiz, L.; Santiago-Hurtado, G.; Moreno-Landeros, V.M.; Olguín-Coca, J.; López-Léon, L.; Bastidas, J.M.; et al. Corrosion behavior of steel-reinforced green concrete containing recycled coarse aggregate additions in sulfate media. *Materials* **2020**, *13*, 4345. [CrossRef]
67. Ojeda, O.; Mendoza, J.M.; Baltazar, M.A. Influence of sugar cane bagasse ash inclusion on compacting, CBR and unconfined compressive strength of a subgrade granular material. *Rev. Alconpat* **2018**, *8*, 194–208.
68. Landa, L.; Márquez, S.; Santiago, G.; Moreno, V.; Mendoza, J.M.; Baltazar, M.A. Effect of the addition of sugar cane bagasse ash on the compaction properties of a granular material type hydraulic base. *Eur. J. Eng. Technol. Res.* **2021**, *6*, 76–79. [CrossRef]
69. *NMX-C-414-ONNCCE-2014. Industria de la construcción—Cementantes Hidráulicos—Especificaciones y Métodos de Ensayo*; ONNCCE S.C.: México City, México, 2014.
70. *ACI 211.1-91. Standard Practice for Selecting Proportions for Normal, Heavyweight, and Mass Concrete*; ACI: Farmington Hills, MI, USA, 2002.
71. *ASTM C33/C33M-16e1. Standard Specification for Concrete Aggregates*; ASTM International: West Conshohocken, PA, USA, 2016.
72. *ASTM C29/C29M-07. Standard Test Method for Bulk Density ("Unit Weight") and Voids in Aggregate*; ASTM International: West Conshohocken, PA, USA, 2007.
73. *ASTM C127-15. Standard Test Method for Relative Density (Specific Gravity) and Absorption of Coarse Aggregate*; ASTM International: West Conshohocken, PA, USA, 2015.
74. *ASTM C128-15. Standard Test Method for Relative Density (Specific Gravity) and Absorption of Fine Aggregate*; ASTM International: West Conshohocken, PA, USA, 2015.
75. Jagadesh, P.; Murthy, A.; Murugesan, R. Effect of processed sugar cane bagasse ash on mechanical and fracture properties of blended mortar. *Constr. Build. Mater.* **2020**, *262*, 120846. [CrossRef]
76. Praveenkumar, S.; Sankarasubramanian, G. Mechanical and durability properties of bagasse ash-blended high-performance concrete. *SN Appl. Sci.* **2019**, *1*, 1664. [CrossRef]
77. Jagadesh, P.; Ramachandramurthy, A.; Murugesan, R.; Prabhu, T.K. Adaptability of sugar cane bagasse ash in mortar. *J. Inst. Eng. India Ser. A* **2019**, *100*, 225–240. [CrossRef]
78. *NMX-C-156-ONNCCE-2010. Determinación de Revenimiento en Concreto Fresco*; ONNCCE S.C.: México City, México, 2010.
79. *ASTM C 1064/C1064M-08. Standard Test Method for Temperature of Freshly Mixed Hydraulic-426 Cement Concrete*; ASTM International: West Conshohocken, PA, USA, 2008.
80. *NMX-C-162-ONNCCE-2014. Determinación de la Masa Unitaria, Cálculo del Rendimiento y Contenido de Aire Del Concreto Fresco Por el Método Gravimétrico*; ONNCCE S.C.: México City, México, 2014.
81. *NMX-C-083-ONNCCE-2014. Determinación de la Resistencia A la Compresión de Especímenes—Método de Prueba*; ONNCCE S.C.: México City, México, 2014.
82. *ASTM G 59-97. Standard Test Method for Conducting Potentiodynamic Polarization Resistance Measurements*; ASTM International: West Conshohocken, PA, USA, 2014.
83. *ASTM A767M-19. Standard Specification for Zinc-Coated (Galvanized) Steel Bars for Concrete Reinforcement*; ASTM International: West Conshohocken, PA, USA, 2019.
84. Yeomans, S.R. Galvanized Steel Reinforcements. In *Corrosion of Steel in Concrete Structures*; Elsevier: Cambridge, MA, USA, 2016; pp. 111–129.
85. Sangoju, B.; Ravindra Gettu, R.; Bharatkumar, B.; Neelamegam, M. Chloride-induced corrosion of steel in cracked OPC and PPC concretes: Experimental study. *J. Mater. Civ. Eng.* **2011**, *23*, 1057–1066. [CrossRef]
86. Pradhan, B. Corrosion behavior of steel reinforcement in concrete exposed to composite chloride–sulfate environment. *Constr. Build. Mater.* **2014**, *72*, 398–410. [CrossRef]
87. *NMX-C-159-ONNCCE-2004. Industria de la Construcción-Concreto-Elaboración y Curado de Especímenes en el Laboratorio*; ONNCCE S.C.: México City, México, 2004.

88. Abdulrahman, A.S.; Mohammad, I. Green plant extract as a passivation promoting inhibitor for reinforced concrete. *Int. J. Eng. Sci. Technol.* **2011**, *3*, 6484–6490.
89. Abdulrahman, A.S.; Mohammad, I. Evaluation of corrosion inhibiting admixtures for steel reinforcement in concrete. *Int. J. Phys. Sci.* **2012**, *7*, 139–143. [CrossRef]
90. Baltazar-Zamora, M.A.; Landa-Ruiz, L.; Rivera, Y.; Croche, R. Electrochemical evaluation of galvanized steel and AISI 1018 as reinforcement in a soil Type MH. *Eur. J. Eng. Res. Sci.* **2020**, *5*, 259–263. [CrossRef]
91. Andrade, C.; Alonso, C. Corrosion rate monitoring in the laboratory and on-site. *Constr. Build Mater.* **1996**, *10*, 315–328. [CrossRef]
92. *ASTM C 876-15. Standard Test Method for Corrosion Potentials of Uncoated Reinforcing Steel in Concrete*; ASTM International: West Conshohocken, PA, USA, 2015.
93. Roventi, G.; Bellezze, T.; Giuliani, G.; Conti, C. Corrosion resistance of galvanized steel reinforcements in carbonated concrete: Effect of wet–dry cycles in tap water and in chloride solution on the passivating layer. *Cem. Concr. Res.* **2014**, *65*, 76–84. [CrossRef]
94. Shaheen, F.; Pradhan, B. Influence of sulfate ion and associated cation type on steel reinforcement corrosion in concrete powder aqueous solution in the presence of chloride ions. *Cem. Concr. Res.* **2017**, *91*, 73–86. [CrossRef]
95. Santiago, G.; Baltazar, M.A.; Galván, R.; López, L.; Zapata, F.; Zambrano, P.; Gaona, C.; Almeraya, F. Electrochemical evaluation of reinforcement concrete exposed to soil Type SP contaminated with sulphates. *Int. J. Electrochem. Sci.* **2016**, *11*, 4850–4864. [CrossRef]
96. Feliu, S.; González, J.A.; Andrade, C. Electrochemical methods for on-site determinations of corrosion rates of rebars. In *Techniques to Assess the Corrosion Activity of Steel Reinforced Concrete Structures*; Berke, N.S., Escalante, E., Nmai, C.K., Whiting, D., Eds.; ASTM STP, 1276; ASTM International: West Conshohocken, PA, USA, 1996; pp. 107–118.
97. Kupwade-Patil, K.; Allouche, E.N. Examination of chloride-induced corrosion in reinforced geopolymer concretes. *J. Mater. Civ. Eng.* **2013**, *25*, 1465–1476. [CrossRef]
98. Badar, M.S.; Kupwade-Patil, K.; Bernal, S.A.; Provis, J.L.; Allouche, E.N. Corrosion of steel bars induced by accelerated carbonation in low and high calcium fly ash geopolymer concretes. *Constr. Build. Mater.* **2014**, *61*, 79–89. [CrossRef]
99. Barrios, C.P.; Baldenebro, F.J.; Núñez, R.E.; Fajardo, G.; Almeraya, F.; Maldonado, E.; Baltazar, M.; Castorena, J.H. Cement Based Anode in the Electrochemical Realkalisation of Carbonated Concrete. *Int. J. Electrochem. Sci.* **2012**, *7*, 3178–3190.
100. Baltazar, M.; Almeraya, F.; Nieves, D.; Borunda, A.; Maldonado, E.; Ortiz, A. Corrosión del acero inoxidable 304 como refuerzo en concreto expuesto a cloruros y sulfatos. *Sci. Tech.* **2007**, *13*, 353–357.
101. Baltazar, M.A.; Santiago, G.; Gaona, C.; Maldonado, M.; Barrios, C.P.; Nunez, R.; Perez, T.; Zambrano, P.; Almeraya, F. Evaluation of the corrosion at early age in reinforced concrete exposed to sulfates. *Int. J. Electrochem. Sci.* **2012**, *7*, 588–600.
102. Landa-Gómez, A.E.; Croche, R.; Márquez-Montero, S.; Villegas Apaez, R.; Ariza-Figueroa, H.A.; Estupiñan López, F.; Gaona Tiburcio, G.; Almeraya Calderón, F.; Baltazar-Zamora, M.A. Corrosion behavior 304 and 316 stainless steel as reinforcement in sustainable concrete based on sugar cane bagasse ash exposed to Na_2SO_4. *ECS Trans.* **2018**, *84*, 179–188. [CrossRef]
103. Baltazar, M.A.; Mendoza, J.M.; Croche, R.; Gaona, C.; Hernández, C.; López, L.; Olguín, F.; Almeraya, F. Corrosion behavior of galvanized steel embedded in concrete exposed to soil type MH contaminated with chlorides. *Front. Mater.* **2019**, *6*, 1–12. [CrossRef]
104. Bellezze, T.; Timofeeva, D.; Giuliani, G.; Roventi, G. Effect of soluble inhibitors on the corrosion behaviour of galvanized steel in fresh concrete. *Cem. Concr. Res.* **2018**, *107*, 1–10. [CrossRef]
105. Figueira, R.M.; Pereira, E.V.; Silva, C.; Salta, M.M. Corrosion protection of hot dip galvanized steel in mortar. *Port. Electrochim. Acta* **2013**, *31*, 277–287. [CrossRef]